Channel Coding for Increased Range Bistatic Backscatter Radio: Experimental Results

Panos N. Alevizos, Nikos Fasarakis-Hilliard, Konstantinos Tountas,
Nikos Agadakos, Nikos Kargas and Aggelos Bletsas
School of Electronic and Computer Engineering,
Technical University of Crete, Chania, Greece 73100
Email: {palevizos, nfasarakis, ktountas, nagadakos, nkargas}@isc.tuc.gr, aggelos@telecom.tuc.gr

***Abstract*—This work offers concrete, low-complexity (small codeword length) channel coding for the bistatic scatter radio channel, complementing the uncoded setup of recent work. The theoretical design is experimentally validated with a commodity software-defined radio (SDR) reader; tag-to-reader ranges up to 134 meters are demonstrated with 13 dBm emitter power, while bit error rate (BER) is reduced or range is increased, on the order of 10 additional meters (or more) compared to the uncoded case, with linear encoding at the tag/sensor and simple decoding at the reader. Even though designing low-complexity channel coding schemes is a challenging problem, this work offers a concrete solution that could accelerate the adoption of scatter radio for large-scale wireless sensor networks, i.e. backscatter sensor networks.**

I. Introduction

Scatter radio, i.e. communication by means of reflection, has been extensively utilized in commercial radio frequency identification (RFID) systems. Current research trends advocate the use of scatter radio in wireless sensing applications (e.g. [1]), where the variable to be sensed (e.g. environmental humidity, soil moisture, mechanical stress or crack) alters the physical properties of an antenna or microwave structure e.g. a delay line; such alteration can be "read" through the signal reflected from the tag/sensor antenna and scattered back towards the reader.

Existing scatter radio sensing testbeds *typically* consist of commercial RFID readers or laboratory measurement apparatus (e.g. sensitive network/spectrum analyzers), where high receiver sensitivity amounts to a non-negligible monetary cost. Furthermore, typical scatter radio systems with *passive* (batterry-less) tags/sensors and monostatic[1] architectures offer limited communication ranges on the order of a few meters.

In an effort to increase communication range, the community has employed energy-assisted (i.e. *semi-passive*) tags, e.g. through the use of a battery [2] or a joint solar-radio frequency harvesting source [3]. Additionally, there is growing intense interest on radio frequency (RF) energy harvesting techniques, including enhancement of rectification efficiency techniques, new rectenna designs and relevant materials (e.g [4] and references therein). Other research directions focused on the appropriate microwave design of the tag antenna front-end, including parameters relevant to reflection coefficients, matching and scattering efficiency, as well as new manufacturing methods [5].

In an effort to *jointly* increase communication range and reduce overall cost, work in [2] proposed a homodyne software-defined monostatic reader, with battery-assisted tags and demonstrated the detection algorithms for non-coherent minimum shift keying (MSK) modulation at the tags; the latter is ideal for the power-limited signal-to-noise-ratio regime (when extended ranges are needed). Subsequent work in [6] analyzed the multiple-access performance of receiver-less tags employing the aforementioned modulation technique and showed that such type of sensor networking is (theoretically) feasible.

Finally, work in [7] proposed a *bistatic* architecture, where carrier emitter and receiver are dislocated, analyzed non-coherent detection algorithms for on-off keying (typically used in commercial RFID systems), as well as frequency-shift keying (FSK) tailored to the bistatic setup. The basic idea in [7] is that *several* ultra low-cost emitters, possibly powered through energy-harvesting techniques, can be stochastically placed in the field to illuminate multiple tag/sensors; thus, the probability of an emitter to be placed relatively close to a tag increases, offering potential link budget gains. Using a commodity relatively-low cost software defined radio (SDR) reader and no channel coding, experimental ranges on the order of 100 meters were demonstrated with the specific non-coherent detectors.

This work attempts to further increase the communication ranges, while keeping the cost at moderate levels. The basic idea is to employ *channel coding* (i.e. error correction) techniques [8], [9] into the bistatic scatter radio setup. Such task may seem formidable: a) any type of processing at the tags must not be highly-complex, otherwise energy consumption at the tags will be prohibitive, b) capacity-approaching codes (e.g. turbo or LDPC codes) typically require extended codeword length i.e. number of bits, which may not be appropriate in sensing applications, and c) there is no standard recipe of applying error-correcting codes to non-coherent designs [10], [11] (and certainly there is no relevant work on channel coding for the bistatic scatter radio channel).

This work offers concrete, low-complexity (small codeword length) channel coding for the bistatic scatter radio channel, complementing the uncoded setup of [7]. In that way, communication range is further increased compared to the uncoded case, offering tremendous potential for new wireless sensor network applications. Section II describes the system model, Sections III, IV describe processing for the uncoded and coded case, respectively, and Section V offers simulation and field experimental results. Work is concluded at Section VI.

[1] i.e. emitter of the carrier (towards the tag) and receiver of the modulated reflected carrier (from the tag) are parts of the same equipment box.

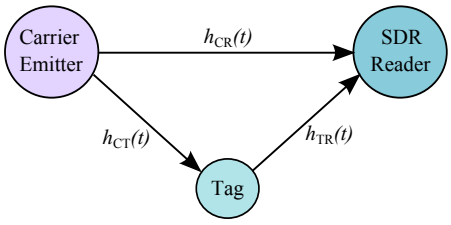

Fig. 1. Bistatic architecture system model: carrier emitter is displaced from SDR reader and RF tag modulates the incident RF signal from carrier emitter.

II. System Model

The bistatic scatter radio architecture is employed, with a carrier emitter, a sensor tag and a software-defined radio (SDR) reader (Fig. 1) [7]; the emitter transmits a carrier at ultra-high frequency (UHF), illuminating a tag. The latter modulates the received carrier by terminating its antenna between two different loads (for binary modulations) and thus, the incident (at the tag) sinusoid wave is reflected with changed phase and amplitude; those two parameters depend on the tag antenna load that is selected each time.

Frequency non-selective (flat) fading is assumed (due to the relatively small communication bandwidth and relatively small channel delay spread), where the *baseband* complex channel impulse response for each of three links is depicted in Fig. 1 and is assumed constant during the channel coherence time T_{coh}:

$$h_l(t) = a_l \ \mathsf{e}^{-\mathrm{j}\phi_l}, \ l \in \{CR, CT, TR\},$$

where $a_{CR}, a_{CT}, a_{TR} \in \mathbb{R}_+$ denote the channel attenuation parameters of the corresponding links and $\phi_{CR}, \phi_{CT}, \phi_{TR}$ stand for the respective phases due to signal propagation delay. The channel impulse response parameters are independent of each other and change independently every T_{coh}.

Carrier emitter transmits a continuous sinusoid wave at carrier frequency F_c; its complex baseband equivalent is given by:

$$c(t) = \sqrt{2P_C} \ \mathsf{e}^{-\mathrm{j}(2\pi\Delta F + \Delta\phi)},$$

where P_C is the carrier transmitting power and ΔF and $\Delta\phi$ model the carrier frequency and carrier phase offset between carrier emitter and SDR reader, respectively. Tag is illuminated by the sinusoid wave $c(t)$, attenuated and rotated due to the channel gain h_{CT}. The tag modulates its information by switching the load at two distinct values (and thus, producing two distinct reflection coefficients Γ_0 and Γ_1) with different rates F_0 and F_1 (F_0 corresponding to bit 0 and F_1 to bit 1).[2] The reflected waveform is attenuated by a constant s, which depends on the tag inherent scattering efficiency. More specifically, the baseband scattered waveform can been written as:

$$x(t) = s \ u_i(t) \ a_{CT} \ \mathsf{e}^{-\mathrm{j}\phi_{CT}} c(t), \ i \in \{0, 1\}. \tag{1}$$

Waveform $u_i(t)$ corresponds to bit $i \in \{0, 1\}$. For FSK modulation and limited receiver bandwidth $W \ll 3F_i$, the waveform is given by [7]:

$$u_i(t) = \Big(v_0 + \frac{4}{\pi}\mathsf{cos}(2\pi F_i t + \Phi_i)\Big)\Pi_T(t), \ i \in \{0, 1\},$$

where $\Pi_T(t)$ is the rectangular pulse of duration T and T denotes the nominal bit duration:

$$\Pi_T(t) \triangleq \begin{cases} 1, & 0 \le t < T, \\ 0, & \text{otherwise.} \end{cases}$$

$\Phi_i \sim \mathcal{U}[0, 2\pi]$ models a random initial phase when bit $i \in \{0, 1\}$ is transmitted and v_0 is a constant that depends on the tag antenna structural mode A_s [13] and the tag reflection coefficients Γ_0, Γ_1.

Thus, for duration T of a single bit, the received baseband signal at the SDR reader is given by:

$$\begin{aligned} y(t) &= a_{CR} \ \mathsf{e}^{-\mathrm{j}\phi_{CR}} c(t) + a_{TR} \ \mathsf{e}^{-\mathrm{j}\phi_{TR}} x(t) + n(t) \\ &= \sqrt{2P_C}\Big(a_{CR} \ \mathsf{e}^{-\mathrm{j}\phi_{CR}} + a_{CT}a_{TR} \ \mathsf{e}^{-\mathrm{j}(\phi_{CT}+\phi_{TR})} s \ u_i(t)\Big) \cdot \\ &\quad \cdot \mathsf{e}^{-\mathrm{j}(2\pi\Delta F + \Delta\phi)} + n(t). \end{aligned} \tag{2}$$

Parameters $\phi_0 = \phi_{CR} + \Delta\phi$ and $\phi_1 = \phi_{CT} + \phi_{TR} + \Delta\phi$ are utilized for simplified notation, as well as $m_0 = \sqrt{2P_C}a_{CR}$, $m_1 = \sqrt{2P_C}a_{CT}a_{TR}\frac{4}{\pi}s$ and $m_2 = \sqrt{2P_C}sv_0$. Therefore, Eq. (2) can be written as:

$$\begin{aligned} y(t) = &\Big(m_0\mathsf{e}^{-\mathrm{j}\phi_0} + \big(m_2\mathsf{e}^{-\mathrm{j}\phi_1} + m_1\mathsf{e}^{-\mathrm{j}\phi_1}\mathsf{cos}(2\pi F_i t + \Phi_i)\big) \cdot \\ &\cdot \Pi_T(t)\Big)\mathsf{e}^{-\mathrm{j}2\pi\Delta F} + n(t). \end{aligned} \tag{3}$$

Carrier frequency offset (CFO) ΔF can be directly estimated using the Fast Fourier transform and periodogram-based techniques [7]. CFO estimation depends on all terms of Eq. (3), including those where no tag information is modulated.[3] After CFO estimation and compensation, the received signal is sampled with sampling period T_s and the baseband signal samples for a bit duration T is given by:

$$\begin{aligned} y[k] \triangleq y(kT_s) = m_0\mathsf{e}^{-\mathrm{j}\phi_0} + \big(m_2\mathsf{e}^{-\mathrm{j}\phi_1} + \\ + m_1\mathsf{e}^{-\mathrm{j}\phi_1}\mathsf{cos}(2\pi F_i k T_s + \Phi_i)\big)\Pi_L[k] + n[k], \end{aligned} \tag{4}$$

with $n[k] = n(kT_s) \sim \mathcal{CN}(0, 2\sigma_n^2)$ and $L \triangleq \frac{T}{T_s}$ the oversampling factor. Notation $\Pi_L[k]$ stands for the oversampled version of $\Pi_T(t)$, i.e.

$$\Pi_L(k) \triangleq \begin{cases} 1, & k = 0, 1, ..., L-1 \\ 0, & \text{otherwise.} \end{cases}$$

The low-pass power spectral density of complex Gaussian process $n(t)$ is given by:

$$S_{nn}(F) = \begin{cases} \frac{N_0}{2}, & |F| \le W \\ 0, & \text{otherwise,} \end{cases}$$

i.e., each noise sample has power $\mathbb{E}[|n[k]|^2] = 2\sigma_n^2 = N_0 W$.

The terms $m_0\mathsf{e}^{-\mathrm{j}\phi_0}$ and $m_2\mathsf{e}^{-\mathrm{j}\phi_1}\Pi_L[k]$ do not contribute any information and can be eliminated with a DC-blocking filter. Thus, after DC-blocking the digital waveform can be written as:

$$\tilde{y}[k] = m_1\mathsf{e}^{-\mathrm{j}\phi_1}\mathsf{cos}(2\pi F_i k T_s + \Phi_i)\Pi_L[k] + n[k], \tag{5}$$

or equivalently, as follows:

$$\begin{aligned} \tilde{y}[k] = \frac{m_1}{2}\Big(\mathsf{e}^{\mathrm{j}(2\pi F_i k T_s + \Phi_i - \phi_1)} + \mathsf{e}^{-\mathrm{j}(2\pi F_i k T_s + \Phi_i + \phi_1)}\Big)\Pi_L[k] \\ + n[k]. \end{aligned} \tag{6}$$

[2] Utilization of more than two loads was recently demonstrated in [12].

[3] Therefore, tag-dependent parameters such as A_s, typically overlooked in the literature, do play important role in the CFO estimation step [7].

The instantaneous carrier-to-signal ratio (CSR) is defined as the instantaneous power ratio between the transmitted carrier power and the *reflected* tag signal power. More specifically:

$$\mathrm{CSR} \triangleq \frac{P_C}{P_T} \triangleq \frac{P_C \pi^2}{P_C 4^2 s^2 |a_{CT}|^2} \implies P_T = \frac{16 s^2 P_C |a_{CT}|^2}{\pi^2}.$$

P_T is the instantaneous tag reflected (i.e. transmitted) power that depends on random amplitude $|a_{CT}|$. The average CSR, $\overline{\mathrm{CSR}}$, is defined the ratio of the average carrier power and the average tag power, i.e. $\overline{\mathrm{CSR}} \triangleq \frac{\pi^2}{16 s^2 \mathbb{E}[|a_{CT}|^2]}$.

The instantaneous received signal-to-noise ratio per bit is defined as:

$$\mathrm{SNR} \triangleq \frac{P_T |a_{TR}|^2}{2\sigma_n^2} L = \frac{8 s^2 P_C}{\pi^2 \sigma_n^2} |a_{CT}|^2 |a_{TR}|^2 L = \frac{m_1^2 L}{4\sigma_n^2},$$

whereas the average received SNR is:

$$\overline{\mathrm{SNR}} = \frac{8 s^2 P_C}{\pi^2 \sigma_n^2} \mathbb{E}[|a_{CT}|^2 |a_{TR}|^2] L. \tag{7}$$

For instance, for $\mathbb{E}[|a_{CT}|^2] = \mathbb{E}[|a_{TR}|^2] = 1$, $\overline{\mathrm{CSR}} = \frac{\pi^2}{16 s^2}$ and $\overline{\mathrm{SNR}} = \frac{8 s^2 P_C}{\pi^2 \sigma_n^2} L$.

III. Uncoded Processing [7]

The received digital signal of Eq. (6) is the sum of two complex exponentials with frequencies $\pm F_i$ and unknown phases $(\Phi_i - \phi_1)$ and $(-\Phi_i - \phi_1)$. If the orthogonality criterion of non-coherent FSK is satisfied, i.e. $|F_1 - F_0| = \frac{k}{T},\ k \in \mathbb{N}$ then any such 2 exponentials of frequencies $\pm F_0$ and $\pm F_1$ will be orthogonal. Consequently, a correlation demodulator can be utilized, since it can exploit the orthogonality property. Specifically, for bit duration T, a bank of demodulators processes the corresponding samples [7]:

$$\begin{aligned} r_0^+ &= \sum_{k=-\infty}^{+\infty} \tilde{y}[k] (\Pi_L[k] \mathsf{e}^{+\mathsf{j}2\pi F_0 k T_s})^* = \sum_{k=0}^{L-1} \tilde{y}[k] \mathsf{e}^{-\mathsf{j}2\pi F_0 k T_s} \\ &= \frac{m_1}{2} \sum_{k=0}^{L-1} \mathsf{e}^{+\mathsf{j}(2\pi(F_i - F_0) k T_s + \Phi_i - \phi_1)} + n_0^+, \end{aligned}$$

where $n_0^+ = \sum_{k=0}^{L-1} n[k] \mathsf{e}^{-\mathsf{j}2\pi F_0 k T_s}$ is the sum of L independent complex Gaussians and thus, it follows complex Gaussian distribution with zero mean and variance $2\sigma_n^2 L$. Similarly, the remaining correlator outputs are given by:

$$\begin{aligned} r_0^- &= \frac{m_1}{2} \sum_{k=0}^{L-1} \mathsf{e}^{-\mathsf{j}(2\pi(F_i - F_0) k T_s + \Phi_i + \phi_1)} + n_0^-, \\ r_1^+ &= \frac{m_1}{2} \sum_{k=0}^{L-1} \mathsf{e}^{+\mathsf{j}(2\pi(F_i - F_1) k T_s + \Phi_i - \phi_1)} + n_1^+, \\ r_1^- &= \frac{m_1}{2} \sum_{k=0}^{L-1} \mathsf{e}^{-\mathsf{j}(2\pi(F_i - F_1) k T_s + \Phi_i + \phi_1)} + n_1^-, \end{aligned}$$

where $n_0^-, n_1^+, n_1^- \sim \mathcal{CN}(0, 2\sigma_n^2 L)$. For non-coherent FSK detection over fading channels, the square law detector is near-optimal except for the case of Rayleigh fading, where it is optimal [14]. Therefore, the following detector is utilized in this work:

$$\begin{aligned} z_0 \triangleq |r_0^+|^2 + |r_0^-|^2 &\overset{\text{bit0}}{\geq} |r_1^+|^2 + |r_1^-|^2 \triangleq z_1 \\ \iff \ln\left(\frac{z_0}{z_1}\right) &\overset{\text{bit0}}{\geq} 0. \end{aligned} \tag{8}$$

Note that the detector above does not require the channel statistics and is solely based on the received information. The above detection test is applied to each symbol of the received sequence.

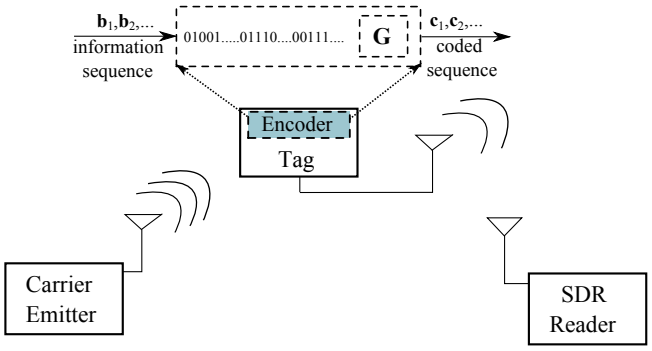

Fig. 2. Encoding at the tag can be directly performed with a matrix multiplication. The latter is straightforward with ultra-low power micro-controller unit (MCU)-based tags.

IV. Channel Coding Processing

A. Encoding

The objective of encoding is to map with an one-to-one function a sequence of k information bits to a sequence of $n \geq k$ coded bits. Since the simplest one-to-one function is a linear function, the encoder can be viewed as the linear function f that maps a k binary tuple to a n binary tuple ($f : \mathbb{B}^k \mapsto \mathbb{B}^n$). Therefore, a linear block code $\mathcal{C}$ over the field $\mathbb{B}$, i.e. the set of all codewords, is a k dimensional subspace of $\mathbb{B}^n$. There exist totally $|\mathbb{B}^k| = 2^k$ binary codewords. Since the dimension of $\mathcal{C}$ is k, there is a set of linearly independent vectors in $\mathbb{B}^n$ that form a basis for the code. Let $\mathbf{g}_1, \mathbf{g}_2, ..., \mathbf{g}_k \in \mathbb{B}^n$ be the row basis vectors for $\mathcal{C}$; then the vectors are placed in a $k \times n$ generation matrix $\mathbf{G}$:

$$\mathbf{G} \triangleq \begin{bmatrix} \mathbf{g}_1 \\ \mathbf{g}_2 \\ \vdots \\ \mathbf{g}_k \end{bmatrix}.$$

It is remarked that a binary n-tuple is a codeword of $\mathcal{C}$, if and only if there exists a binary k-tuple that can generate this n-tuple from $\mathbf{G}$, i.e.

$$\mathbf{c} \in \mathcal{C} \iff \exists\ \mathbf{b} \in \mathbb{B}^k : \mathbf{c} = \mathbf{b}\mathbf{G}. \tag{9}$$

The ratio $r \triangleq \frac{k}{n}$ defines the rate of the code, while the minimum distance $d_{\min}^{\mathcal{C}}$ of a code $\mathcal{C}$ is the smallest Hamming weight (i.e. the number of non-zero components) of any codeword in $\mathcal{C}$, except the all zero codeword:

$$d_{\min}^{\mathcal{C}} = \min_{\mathbf{c} \in \mathcal{C} \setminus \{\mathbf{0}\}} w_{\mathrm{H}}(\mathbf{c}).$$

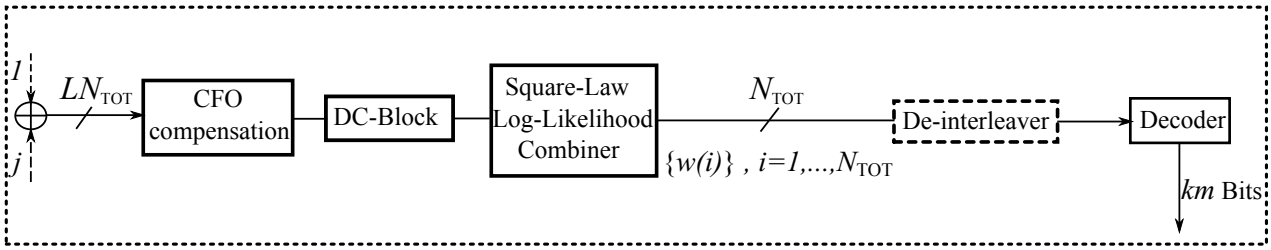

Fig. 3. Complete signal processing chain with channel coding for non-coherent FSK in bistatic backscatter radio.

A code $\mathcal{C}$ is usually briefly described by the triplet $(n, k, d^{\mathcal{C}}_{\min})$ that affects its properties.

Therefore, encoding of k bits that produce n coded bits is performed at the tag by a simple multiplication with the generation matrix, as described by Eq. (9). The latter can be stored in the tag memory and can be directly implemented in ultra-low power, micro-controller unit (MCU)-based tags, as those used in this work. The spatial complexity of this procedure is $\mathcal{O}(k \cdot n)$, however, it can be $\mathcal{O}(n)$ if more sophisticated coding schemes are utilized. The coded bits can be then reflected in the same way as with uncoded bits. Nevertheless, with resource-constrained tags, memory is not unlimited and n, k should be both kept relatively small, as discussed below.

B. Decoding with Non-Coherent FSK

The idea of decoding is to exploit the information redundancy that has been introduced by the encoder in order to increase the reliability of reception, at the cost of the reduction in transmission rate. The classic maximum likelihood decoders perform joint detection and decoding (by trying to minimize the probability of decoding error); however, in non-coherent FSK modulation, closed form expressions for maximum likelihood (ML) decoding cannot be derived except for the case of Rayleigh fading [14]. Unfortunately, in bistatic backscatter radio there are additional channel parameters that must be eliminated compared to classic radio architectures. Therefore, a near-optimal low-complexity decoder must be carefully derived. The sub-optimal decoder assumes that a square law detector precedes, and thus, its input is the (soft) output of the square law detector. In such coded setup, the detector does not perform final detection, and thus, it is renamed as square-law likelihood-ratio combiner (SLLRC).

The output of the SLLRC produces $N_{\mathrm{TOT}} = m \cdot n$ symbol samples that correspond to N_{TOT} transmitted coded bits, where n is the length of the code and $m \in \mathbb{N}$ (i.e., it is assumed without loss of generality, that the length of the packet N_{TOT} is multiple of the length of the code). The SLLRC passes the soft information $\mathsf{ln}\left(\frac{z_0}{z_1}\right)$ to the decoder for each received coded symbol. Let

$$\{w(i)\}_{i=1}^{N_{\mathrm{TOT}}} \triangleq \left\{ \mathsf{ln}\left(\frac{z_0(i)}{z_1(i)}\right) \right\}_{i=1}^{N_{\mathrm{TOT}}}. \tag{10}$$

The real number $w(i),\ \forall i$, is the soft information for symbol i. The sign of $w(i)$ is the hard decision information for symbol i, while the absolute of $w(i), |w(i)|$, is the reliability of symbol i. A detector that does not utilize decoding ($k = n$), uses only the hard decision information to infer the value of symbol i and acts independently for each $i \in \{1, ..., N_{\mathrm{TOT}}\}$, i.e. as in Eq. (8). On the other hand, the decoder processes n-tuples of the whole sequence of $\{w(i)\}_{i=1}^{N_{\mathrm{TOT}}}$ and finds the most probable codeword that corresponds to that sequence. This process is repeated m times where the output of decoder produces an estimation of the $k \cdot m$ information bits.

The near-ML decoder needs the knowledge of the whole code i.e., each coded bit j (out of n) of codeword i (out of 2^k) of code $\mathcal{C} \triangleq \{c_{i,j}\}_{i=1,j=1}^{2^k,n}$. The size of the code is $n \cdot 2^k$ bits. The decoder uses a linear operator on the code in order to convert the bits with values 0 or 1 to symbols with values ± 1. Specifically, since $w(i) \geq 0 \implies$ bit 0 and $w(i) < 0 \implies$ bit 1, the following operation is utilized that converts $c_{i,j}$ to $a_{i,j}$:

$$\mathcal{A} = \{a_{i,j}\}_{i=1,j=1}^{2^k,n} \triangleq \{-2c_{i,j} + 1\}_{i=1,j=1}^{2^k,n} \tag{11}$$

i.e. bit 0 ($w(i) \geq 0$) is mapped to symbol $+1$ and bit 1 is mapped to symbol -1 ($w(i) < 0$). Note that the values $+1$ and -1 are arbitrary, without optimality loss, since the offered decoder is invariant under scaling with a positive number. Finally, the decoder searches for the closest codeword in terms of Euclidean distance. Let $\mathbf{w}_l \triangleq \big[w\big(1 + (l-1)m\big)\ w\big(2 + (l-1)m\big)\ ....\ w\big(n + (l-1)m\big)\big]$ and $\mathbf{a}_i \triangleq [a_{i,1}\ a_{i,2}\ ...\ a_{i,n}]$ then

$$\hat{\mathbf{v}}_l = \underset{\mathbf{a}_i \in \mathcal{A}}{\arg\min}\ ||\mathbf{a}_i - \mathbf{w}_l||_2^2,\ l = 1, ..., m. \tag{12}$$

$\hat{\mathbf{v}}_l$ is an estimation of the l-th transmitted codeword ($l = 1, ..., m$). The corresponding information bit sequence $\hat{\mathbf{b}}_l$ can be extracted from $\hat{\mathbf{v}}_l$.

The above optimization problem can be easily shown to have exponential complexity on the dimension of the code k (due to the exhaustive search on all possible n-tuples of set $\mathcal{A}$). However, if small length n is utilized, then Eq. (11) can be computed with low computational complexity cost. For simulation as well as experimental results, Reed-Muller codes with small length and good error correction capabilities [8], [9] are studied in this work. Fig. 3 depicts the whole signal processing chain of non-coherent FSK with channel coding in bistatic backscatter radio. The de-interleaving block is optional and is explained below.

C. Coding Gain with Interleaving

In fading environments, errors usually occur in long bursts due to deep fading events. In bistatic backscatter radio, deep fading events are even more frequent due to the product of

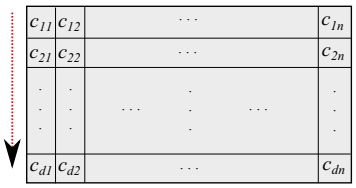

Fig. 4. With interleaving, d codewords are stored at the encoder and bits are transmitted column-wise. In that way, burst of errors due to fading affect bits of different codewords and not consecutive bit of the same codeword.

channel gain terms a_{CT}, a_{TR}. The use of channel codes with small block length cannot overpass the deep fading event, due to their small bit error-correction capability.

In order to overpass this difficulty, the interleaving technique could be employed, in conjunction with linear block codes (of relatively small length). The transmitter stores a block of d codewords for transmission and transmits the information column-wise, i.e. it transmits consecutively the first coded bit of each of the d codewords and then the second bit of each of the d codewords and so forth, until the n-th coded bit (Fig. 4). The receiver stores $d \cdot n$ received symbols (in a $d \times n$ matrix) and performs decoding row-wise, i.e it decodes symbol sequences that correspond to actual codewords. With interleaving, the burst errors affect bits of different codewords rather than consecutive bits of the same codeword.

Parameter d is the interleaving depth of the interleaver and it can be proved that as parameter d increases, the linear block code can achieve diversity of order $d^{\mathcal{C}}_{\min}$ [11]. The choice of d usually depends on the application and the corresponding channel coherence time $T_{\rm coh}$. Despite its attractive flavor, the main drawback of this technique is the added delay at both transmitter and receiver side, since they must both store in their memory d codewords before transmission or reception processing, respectively.

V. Numerical Results

Fig. 5 illustrates the bit error rate (BER) performance as a function of average received SNR for the bistatic backscatter radio setup of Fig. 1, where each of the three channel links suffers from Rayleigh fading. Simulations test the following: (a) uncoded non-coherent FSK detector of Eq. (8), as well as (b) coded non-coherent FSK with Reed Muller (RM) channel code $\mathcal{C}_{\rm RM}$ and parameters $(32, 16, 8)$.[4] The processing chain of Fig. 3 is utilized with interleaving depths $d = 16, 32, 64$ and decoder of Eq. (12). The channel coherence time is assumed to span 128 bit periods in both scenarios and the oversampling factor was set to $L = 100$. The average CSR was set $\overline{\rm CSR} = 20$dB. In both cases (coded and uncoded), perfect synchronization and CFO compensation were assumed.

It is remarked that despite the small block length and the sub-optimal decoder of Eq. (12), the coded schemes achieve better bit error rate capability and offer significant coding gain, as the average SNR increases. Specifically at BER $= 10^{-2}$, depth $d = 16$ of interleaving with channel coding has a gain of 8dB, while depth $d = 64$ interleaving offers gain of 13dB. However, the transmission rate has been halved (compared to the uncoded case), since $r = \frac{16}{32} = \frac{1}{2}$. This result shows that the tag-reader range at which reliable communication exists, can be further increased if channel codes of small block length and small implementation complexity are employed at the tag, in conjunction with the proposed simple decoder.

[4]The specific code has the best coding gain over all Reed-Muller codes up to length $n = 32$ (Table I columns 2-3 in [9]).

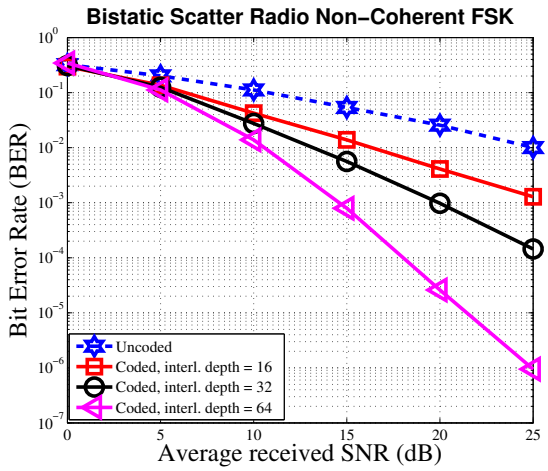

Fig. 5. BER performance as a function of average received SNR for non-coherent FSK in bistatic backscatter radio system model with or without *channel coding* and interleaving depth d.

A. Experimental Results: Achieved Ranges

Ranging measurements were conducted outdoors. A carrier emitter was utilized with +13dBm transmission power at 867MHz. A programmable, semi-passive RF tag (based on a 8-bit ultra-low power micro-controller unit from Silicon Laboratories) was used to modulate the reflected carrier with FSK modulation at 1kbps bit-rate. Reception was implemented with a commodity USRP software defined radio (SDR) and a laptop PC, running the reception processing algorithms in software. Omnidirectional antennas were employed on both emitter, tag and SDR reader. For the uncoded setup, a packet of 62 preamble bits (known to receiver for synchronization) plus 32 information bits was utilized, whereas for the coded setup, the packet consisted of 62 preamble bits plus 64 coded bits. The coded system employed a $(32, 16, 8)$ Reed-Muller code with interleaving depth $d = 2$.

Three different scenarios were studied, depicted at Figs. 7, 8, 9. In scenario 1, tag was located between carrier emitter and reader (Fig. 7), in scenario 2, the carrier emitter was placed between tag and reader, so that the tag-to-reader distance was larger than emitter-to-reader distance (Fig. 8). Finally, in scenario 3 the tree terminals formed a rectangle (Fig. 9).

Table I offers the achieved ranges from the experimental tests (Fig. 6); it is found that for the specific setup, the offered tag-to-reader ranges can be increased by at least 6 meters for scenario 1 and 14 meters for scenario 3, using the low-complexity, small block-length channel codes with the proposed simple decoder. Equivalently, for similar ranges, the proposed processing with channel coding offers more reliable communication, compared to the uncoded case, as expected. In fact, ranges on the order of hundreds of meters are feasible, corroborating the idea of bistatic backscatter radio for wireless sensor network applications; a large number of stochastically-placed emitters, potentially power through energy harvesting

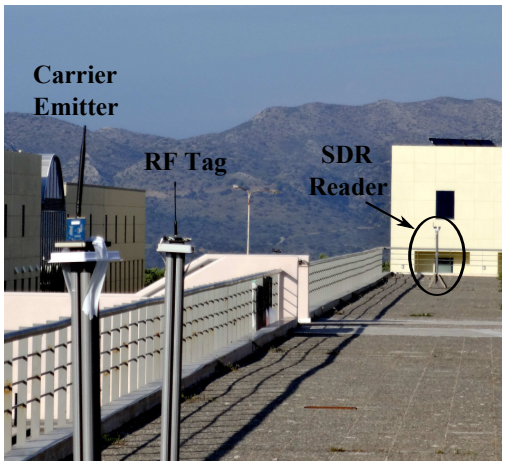

Fig. 6. Bistatic experimental setup for backscatter radio.

techniques could illuminate a sheer number of tags that reflect their signals towards one (or more) SDR readers. In that way, a large geographical area can be served and this work is a small step forward towards the realization of that vision.

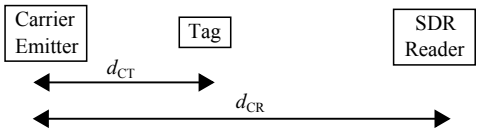

Fig. 7. Scenario 1: Tag between carrier emitter and reader.

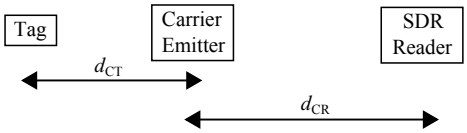

Fig. 8. Scenario 2: Carrier emitter between tag and reader.

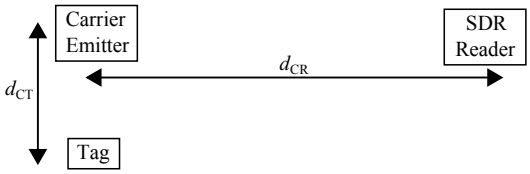

Fig. 9. Scenario 3: 90 degrees angle between tag - carrier emitter and carrier emitter - reader.

TABLE I. BER PERFORMANCE FOR DIFFERENT SCENARIOS

Scenario	d_{CR}	d_{CT}	d_{TR}	BER coded	BER uncoded
1	134 m	2.8 m	**131.2** m	3.03%	$> 15\%$
1	128 m	2.8 m	**125.2** m	0%	6.4%
2	128 m	4.8 m	**132.8** m	3.24%	12.11%
3	134 m	2.6 m	**134.025** m	5.07%	$> 15\%$
3	120.4 m	2.6 m	**120.43** m	0%	8.04%

VI. CONCLUSION

This work presented concrete channel coding for the bistatic scatter radio channel, for non-coherent binary FSK modulation. Tag-to-reader ranges up to 134 meters were experimentally demonstrated with 13 dBm emitter power, while bit error rate (BER) reduction or range increase, on the order of 10 additional meters were offered (or more compared to the uncoded case), with linear encoding at the tag/sensor and simple decoding at the reader. Even though low-complexity channel coding is by itself a great challenge, this work offered a concrete, simple solution that could further leverage the adoption of scatter radio in large-scale, ultra-low cost wireless sensor networks.

ACKNOWLEDGMENT

This work was supported by the ERC-04- BLASE project, executed in the context of the "Education & Lifelong Learning" Operational Program of the National Strategic Reference Framework (NSRF), General Secretariat for Research & Technology (GSRT), funded through European Union-European Social Fund and Greek national funds.

REFERENCES

[1] J. Virtanen, L. Ukkonen, T. Björninen, A. Z. Elsherbeni, and L. Sydänheimo, "Inkjet-Printed Humidity Sensor for Passive UHF RFID Systems," *IEEE Trans. Instrum. Meas.*, vol. 60, no. 8, pp. 2768–2777, Aug. 2011.

[2] G. Vannucci, A. Bletsas, and D. Leigh, "A software-defined radio system for backscatter sensor networks," *IEEE Trans. Wireless Commun.*, vol. 7, no. 6, pp. 2170–2179, Jun. 2008.

[3] A. Collado and A. Georgiadis, "Conformal Hybrid Solar and Electromagnetic (EM) Energy Harvesting Rectenna," *IEEE Trans. Circuits Syst. I*, vol. 60, pp. 2225–2234, Aug. 2013.

[4] N. B. Carvalho et al, "Wireless Power Transmission: R&D Activities within Europe," *IEEE Trans. Microw. Theory Tech.*, 2014, to appear, available online.

[5] V. Lakafosis, A. Rida, R. Vyas, L. Yang, S. Nikolaou, and M. M. Tentzeris, "Progress towards the first wireless sensor networks consisting of inkjet-printed, paper-based RFID-enabled sensor tags," *Proc. IEEE*, vol. 98, no. 9, pp. 1601–1609, Sep. 2010.

[6] A. Bletsas, S. Siachalou, and J. N. Sahalos, "Anti-collision backscatter sensor networks," *IEEE Trans. Wireless Commun.*, vol. 8, no. 10, pp. 5018–5029, Oct. 2009.

[7] J. Kimionis, A. Bletsas, and J. N. Sahalos, "Increased range bistatic scatter radio," *IEEE Trans. Commun.*, vol. 62, no. 3, pp. 1091–1104, Mar. 2014.

[8] S. Lin and D. J. Costello, *Error Control Coding* , 2nd ed. Prentice Hall, Jun. 2004.

[9] G. D. Forney Jr., "Introduction to binary block codes," MIT, 2005, principles of Digital Communication II.

[10] A. G. I. Fàbregas and A. J. Grant, "Capacity approaching codes for non-coherent orthogonal modulation," *IEEE Trans. Wireless Commun.*, vol. 6, no. 11, pp. 4004–4013, Nov. 2007.

[11] J. G. Proakis and M. Salehi, *Digital Communications*, 5th ed. Upper Saddle River, NJ, USA: Prentice-Hall, November 2007.

[12] S. Thomas, E. Wheeler, J. Teizer, and M. Reynolds, "Quadrature amplitude modulated backscatter in passive and semipassive UHF RFID systems," *IEEE Trans. Microw. Theory Tech.*, vol. 60, no. 4, pp. 1175–1182, Apr. 2012.

[13] A. Bletsas, A. G. Dimitriou, and J. N. Sahalos, "Improving backscatter radio tag efficiency," *IEEE Trans. Microw. Theory Tech.*, vol. 58, no. 6, pp. 1502–1509, Jun. 2010.

[14] W. E. Stark, "Capacity and cutoff rate of noncoherent FSK with nonselective Rician fading," *IEEE Trans. Commun.*, vol. 33, no. 11, pp. 1153–1159, Nov. 1985.